Hindawi Publishing Corporation
Journal of Nanomaterials
Volume 2014, Article ID 345845, 12 pages
http://dx.doi.org/10.1155/2014/345845

Research Article

Hyaluronate Targeted Solid Lipid Nanoparticles of Etoposide: Optimization and *In Vitro* Characterization

Jaleh Varshosaz,[1] Parviz Mohammadi Ghalaei,[1] and Farshid Hassanzadeh[2]

[1] *Department of Pharmaceutics, School of Pharmacy and Novel Drug Delivery Systems Research Centre, Isfahan University of Medical Sciences, P.O. Box 81745-359, Isfahan, Iran*
[2] *Department of Medicinal Chemistry, School of Pharmacy and Novel Drug Delivery Systems Research Centre, Isfahan University of Medical Sciences, P.O. Box 81745-359, Isfahan, Iran*

Correspondence should be addressed to Jaleh Varshosaz; varshosaz@pharm.mui.ac.ir

Received 13 October 2013; Revised 25 January 2014; Accepted 10 February 2014; Published 18 March 2014

Academic Editor: Renyun Zhang

The aim of the present study was preparation of hyaluronan (HA) targeted solid lipid nanoparticles (SLNs) of etoposide. SLNs were prepared by an emulsification-solvent evaporation method and physically coated with HA. Four variables, including the ratio of cetyl alcohol to cationic lipid, cationic lipid type (stearylamine (SA) or dodecylamine (DDA)), lipid to HA ratio, and organic to aqueous phase ratio, were studied in an irregular fraction factorial design. Four responses, including particle size, zeta potential, drug loading, and 24-hour release efficiency percent, were measured for each formulation and then the optimization was carried out. The percent of HA coated on the SLNs was calculated by CHN elemental analysis which was shown to be about 55.89%. The cationic lipid type and the ratio of cetyl alcohol to cationic lipid had the highest influence on particle size and zeta potential, respectively. The highest effects of the ratio of lipid to HA and the organic to aqueous phase ratio were on the drug loading efficiency of SLNs. The optimized formulation of SLNs was obtained by SA, the equal proportion of cetyl alcohol and cationic lipid, the ratio of 1.5 for lipid to HA, and 10% of organic phase to aqueous phase.

1. Introduction

Etoposide (VP-16) is a hydrophobic anticancer agent inhibiting topoisomerase II. Unfortunately, despite its appropriate solubilization in vehicle solvents, its poor bioavailability concurs to disappointing results requiring the development of new delivery system forms. Etoposide is used in the treatment of ovarian cancer [1], small cell carcinoma [2], non-Hodgkin's lymphoma [3], Hodgkin's lymphoma [4], and acute myelogenous lymphoma [5], with or without other drugs. This drug as other chemotherapy agents has many side effects such as bone marrow suppression, granulocytopenia, thrombocytopenia [6], and gastrointestinal toxicity such as nausea, vomiting, diarrhea, mucositis, moderate to severe esophagitis, hepatotoxicity accompanied by increase in bilirubin and hepatic enzymes, metabolic acidosis, and anemia [7].

Nanoparticles are one of the most promising ways in decreasing side effects of anticancer drugs. After injecting the nanoparticles, they tend to accumulate in tumor tissue. This phenomenon owes to more ratios of endocytosis in cancerous cells than healthy cells.

Solid lipid nanoparticles (SLNs) that are often considered for intravenous use are colloidal submicron carriers sized 50 to 1000 nm, composed of solid lipids dispersed in water or surfactant aqueous solutions. These nanoparticles have particular features like small size, high surface of contact, and high loading of drug that makes them as potential and beneficial carriers for improving drug efficacy [8, 9].

SLNs are similar to o/w emulsions used for total parenteral nutrition, with the difference that emulsion liquid lipid has been replaced with a solid lipid. SLNs have advantages such as controlled drug release in considered site, excellent biocompatibility, increase in drugs' stability, high drug content, easy industrialization and sterilization, better control on drug release kinetics, high bioavailability for bioactive drugs, chemical protection of sensitive drugs, easier producing process compared to bio-polymeric nanoparticles,

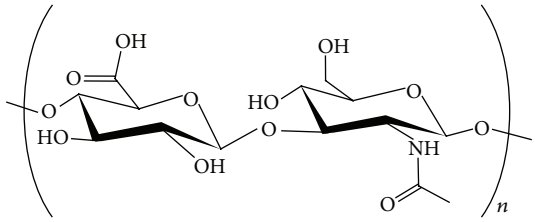

Figure 1: Chemical structure of hyaluronan: polymeric repeat of *D*-glucuronic acid and *N*-acetylglucosamine.

being producible by common emulsification methods, long-time stability, and various applications [10–12].

There are some reports on the successful production of etoposide containing nanoparticles. In a study [3], etoposide formulated as an injectable solution (Teva) was loaded into all-biocompatible poly(lactide-co-glycolide) (PLGA) or PLGA/Pluronic188-blended nanoparticles. Obtained results suggest that the use of PLGA and PLGA/Pluronic188 nanoencapsulation over preexisting etoposide formulation could induce a greatly improved cytotoxic activity. Yadav et al. [13] prepared PLGA-monomethoxy-poly(polyethylene glycol) and PLGA-Pluronic copolymers and Reddy et al. [14] worked on nanoparticles produced by tripalmitin and the tumoricidal effects of etoposide incorporated into lipid nanoparticles after single-dose administration were investigated in Dalton's lymphoma ascites bearing mice. The frequency of dead cells treated with the nanoparticulate formulations remained high even after 8 days of treatment compared with free etoposide. This study signified the advantage of incorporating etoposide into tripalmitin nanoparticles in controlling its biodistribution and enhancing the tumor uptake by several folds. Nanoparticles were administered from three different routes of subcutaneous, intraperitoneal, and intravenous routes; among them subcutaneous injection was the route of preference for facilitating high tumor uptake and retention and was likely to have a greater antitumor effect resulting in tumor regression [15].

Etoposide formulated with poly(butyl cyanoacrylate) nanoparticles and polysorbate 80 exhibited the highest cytotoxicity toward adenocarcinoma cells [16]. Another type of nanoparticles used in the delivery of etoposide is reported by Kiliay et al. [17] who used the natural polymer of poly(3-hydroxybutyrate-co-3-hydroxyhexanoate), as a base matrix for the production of etoposide nanoparticles. They used folic acid as a ligand on the nanoparticles for targeted delivery of this drug in HeLa cells.

Hyaluronan (HA) (Figure 1), available in the market as sodium hyaluronate, is a high molecular weight glycosaminoglycan present in the extracellular matrix and is necessary for cellular growth, structural stability of organs, and tissue structure. HA regulates cell proliferation and movements by interacting with CD44 receptors (its main receptors) and receptor for HA mediated motility (RHAMM) [18].

Because of high expression of CD44 by cancer cells, targeting of drugs to CD44 by HA is an effective strategy to treat cancers. HA as bound to the nanoparticles, in addition to its targeting roll, can protect from nanoparticles against body phagocytosis system [19–21]. This ligand has been used in different nanoparticulate delivery systems for chemotherapeutic agents such as doxorubicin [22], epirubicin [23], paclitaxel [24], mitomycin C [25], siRNA [26], and DNA [27]. To our knowledge, there is no report on the use of HA targeted SLNs for delivery of etoposide. For this purpose the aim of the present study was the preparation, characterization, and optimization of HA targeted SLNs of etoposide.

Table 1: Description and trial levels of studied factors in irregular fraction factorial design used in preparation of etoposide loaded in SLNs.

Studied variables	Level	
	I	II
C: cetyl alcohol/amine ratio	1	2
L: lipid/HA ratio	1.5	3
A: amine type	Dodecylamine (DDA)	Stearylamine (SA)
O: organic/aqueous phase (%)	10	20

2. Materials and Methods

2.1. Materials. Stearylamine (SA), dodecylamine (DDA), and cetyl alcohol were all from Sigma-Aldrich Company (US). Acetone, dichloromethane, dialysis bags with molecular weight cut-off of 12,400 Da, and Tween 80 were from Merck Chemical Company (Germany). Etoposide was a gift from Nippon Kayaku Co., Ltd. (Tokyo, Japan), and sodium hyaluronate (Mw = 6,400 Da) was provided by Lifecore Biomedicals (US).

2.2. Experimental Design of Study. Four variables, including the ratio of cetyl alcohol to cationic lipid, cationic lipid type, lipid to HA ratio, and organic to aqueous phase ratio, were studied, each with 2 levels in an irregular fraction factorial design (Table 1) by Design-Expert software (version 7.0.0; Stat-Ease, Inc., Minneapolis, MN, USA).

Twelve different formulations were proposed (Table 2). Four responses, including particle size, zeta potential, drug loading efficiency percent, and 24-hour release efficiency percent, were measured for each formulation. Nontargeted and targeted SLNs were compared for their physicochemical properties.

2.3. Manufacturing of SLNs. SLNs were produced by emulsification-solvent evaporation method. The lipid phase, including 30 mg of etoposide and 60 mg of lipids consisting of cetyl alcohol and SA or DDA, was dissolved in 1.8 or 3.6 mL of the 1 : 1 mixture of acetone-dichloromethane. Then this solution was added during 3 minutes to 18 mL of deionized water containing 1 w/v% of Tween 80 while being stirred at 1200 RPM. Ultimately, produced nanoemulsion was stirred in 600 RPM at room temperature for 75 minutes in order to evaporate the organic solvents [28]. The blank nanoparticles

Table 2: Different formulations of SLNs loaded with etoposide proposed by Design-Expert software according to an irregular fraction factorial design.

Formulation code	Cetyl alcohol/amine ratio	Lipid/HA ratio	Amine type	Organic/aqueous phase percent
$C_2L_{1.5}DO_{20}$	2	1.5	DDA	20
$C_1L_3SO_{20}$	1	3	SA	20
$C_1L_3DO_{20}$	1	3	DDA	20
$C_2L_3DO_{10}$	2	3	DDA	10
$C_1L_3SO_{10}$	1	3	SA	10
$C_1L_{1.5}SO_{10}$	1	1.5	SA	10
$C_1L_{1.5}DO_{20}$	1	1.5	DDA	20
$C_2L_{1.5}SO_{20}$	2	1.5	SA	20
$C_1L_{1.5}DO_{10}$	1	1.5	DDA	10
$C_2L_3DO_{20}$	2	3	DDA	20
$C_2L_3SO_{10}$	2	3	SA	10
$C_2L_{1.5}SO_{10}$	2	1.5	SA	10

were produced by the same method, but without adding etoposide.

2.4. Physical Binding of HA to the Surface of SLNs. In order to produce targeted nanoparticles after 15 minutes of adding the organic phase to aqueous phase of the nanoemulsion dispersion, HA was dissolved in deionized water containing Tween 80 (1 w/v%) and added to the mixture of nanoparticles during 5 minutes while being stirred at 600 RPM [29].

Unbound HA was separated from nanoparticles mixture by dialyzing the SLNs suspension against 100 mL of deionized water containing 1 w/v% of Tween 80 using a dialysis bag with molecular weight cut-off of 12,400 Da for 40 minutes and the dialysis solution was replaced every 10 minutes.

2.5. Measuring the Particle Size, Polydispersity Index, and Zeta Potential of SLNs. The particle size, polydispersity index, and zeta potential of nanoparticles were measured by a Zetasizer (Zetasizer 3000; Malvern Instruments, Malvern, UK), after 1 : 10 dilution of the samples with deionized water.

2.6. Determining Drug Loading Efficiency in SLNs. The loading efficiency percent of HA targeted SLNs was determined by centrifugation (Eppendorf 5430 centrifuge, Germany) using centrifugal filter tubes (Amicon Ultra, Ireland) with a 10 kDa molecular weight cut-off to separate the aqueous medium [30]. The concentration of free etoposide in the filtrate was determined by measuring its absorbance in 276.4 nm by a UV-VIS spectrophotometer (Shimadzu Scientific Instruments, Japan) and converting the absorbance to concentration using the absorption equation ($y = 0.005x + 0.031$) of etoposide in aqueous solution of Tween 80 (1 w/v%). The amount of encapsulated drug was computed indirectly by calculating the difference between the total amounts of drug used to prepare the formulations. Ultimately, the loading efficiency percent was computed by the following equation:

$$\text{Loding efficiency percent} = \frac{(\text{Total drug weight} - \text{Free drug weight})}{\text{Total drug weight}} \times 100. \quad (1)$$

2.7. Determining Drug Release Efficiency. Drug release profiles from the nanoparticles were determined in phosphate buffer saline (PBS, 0.01 M, pH 7.4 containing 1 w/v% of Tween 80) at 37°C. A total of 2 mL of HA coated nanoparticles suspension was placed in dialysis bags with molecular weight cut-off of 12,400 days and the bag was then completely submerged in a beaker containing 50 mL of PBS on a magnetic stirrer with a speed of 200 RPM. Samples were withdrawn periodically and replaced with the same volume of PBS at the same temperature. The content of etoposide in the samples was determined spectrophotometrically by measuring their absorbance in 268.7 nm from the equation of $y = 0.003x + 0.016$. The data were expressed as the mean value of 3 independent experiments. The parameter of release efficiency within 24 hours ($RE_{24}\%$) was used to compare the release profiles:

$$RE_{24}\% = \frac{\int_0^{24} y \cdot dt}{y100 \cdot t} \times 100. \quad (2)$$

2.8. Optimization of the Formulation of HA Targeted SLNs. The gathered data for responses were analyzed by Design-Expert software and the optimum formulation was suggested by the software. The constraints of particle size were $395.6 \leq Y_1 \leq 804.7$ nm with particle size targeted on minimum; for zeta potential it was $-13.74 \leq Y_2 \leq -1.35$ mV while its absolute value was desired to be maximized; for loading efficiency the constraints were $37.84 \leq Y_3 \leq 66.58\%$ with the goal set at the maximum and $RE_{24}\%$ had constraints of $52.89 \leq Y_4 \leq 69.06\%$ with desired target set at the maximum.

Table 3: Particle size and polydispersity index (PdI) of nontargeted and HA targeted SLNs ($n = 3$).

Formulation code	Particle size (nm) ± SD		Polydispersity index (PdI) ± SD	
	Nontargeted	HA targeted	Nontargeted	HA targeted
$C_2L_{1.5}DO_{20}$	400.3 ± 29.5	620.9 ± 48.3	0.309 ± 0.035	0.493 ± 0.053
$C_1L_3SO_{20}$	211.8 ± 22.3	406.3 ± 36.2	0.226 ± 0.038	0.342 ± 0.065
$C_1L_3DO_{20}$	525.1 ± 44.9	712.4 ± 85.9	0.602 ± 0.041	0.812 ± 0.069
$C_2L_3DO_{10}$	336.2 ± 36.2	488.2 ± 72.3	0.485 ± 0.028	0.764 ± 0.058
$C_1L_3SO_{10}$	219.3 ± 33.1	409.1 ± 43.7	0.294 ± 0.047	0.369 ± 0.061
$C_1L_{1.5}SO_{10}$	187.3 ± 14.5	411.6 ± 28.1	0.165 ± 0.023	0.287 ± 0.044
$C_1L_{1.5}DO_{20}$	493.5 ± 38.3	790.5 ± 66.4	0.343 ± 0.033	0.674 ± 0.049
$C_2L_{1.5}SO_{20}$	299.9 ± 45.7	507.3 ± 61.8	0.317 ± 0.061	0.358 ± 0.082
$C_1L_{1.5}DO_{10}$	528.5 ± 61.7	804.7 ± 79.5	0.584 ± 0.052	0.719 ± 0.078
$C_2L_3DO_{20}$	300.2 ± 47.8	452.6 ± 69.1	0.407 ± 0.062	0.790 ± 0.088
$C_2L_3SO_{10}$	250.4 ± 49.7	395.6 ± 57.1	0.361 ± 0.064	0.512 ± 0.073
$C_2L_{1.5}SO_{10}$	214.1 ± 51.2	427.2 ± 71.7	0.426 ± 0.053	0.548 ± 0.085

2.9. Morphology Study. Morphology of the nanoparticles was characterized by scanning electron microscopy (SEM). The nanoparticles were mounted on aluminum stabs, sputter-coated with a thin layer of Au/Pd, and examined using an SEM (Philips XL30, Almelo, The Netherlands).

2.10. Determining the Amount of Hyaluronate Bound on the Surface of the SLNs. After separation of unbound HA, some part of the targeted nanoparticles mixture was dried under vacuum and subjected to elemental analysis (CHN) (CHNS-932, Leco, USA) in order to determine the percentage of HA coated on the sample. By subtracting the total amount of HA from gaining value, the amount of HA bound on the SLNs surface was calculated.

3. Results and Discussion

3.1. Particle Size of SLNs. Table 3 shows mean particle size and polydispersity index for each formulation.

3.1.1. Nontargeted SLNs. As it could be observed in Table 3 the formulations $C_1L_{1.5}SO_{10}$ and $C_1L_{1.5}DO_{10}$ had the smallest and the largest particle sizes among nontargeted SLNs, respectively. In the current study, it is observed that SLNs produced from SA had smaller particle size than DDA containing ones (Figure 2). This owes probably to longer chain of SA that is more miscible with cetyl alcohol. SA has 18 carbon atoms, cetyl alcohol is C16, and DDA is C12. Therefore, as SA is structurally more similar to the lipid phase of cetyl alcohol compared to DDA, it is more miscible in the lipid phase. Similar results have been obtained in studies by Kremser et al. [20] and Sun [21].

Increase in cetyl alcohol/amine ratio in DDA containing SLNs caused decrease in particle size (Figure 2), which could be because of the low miscibility of the DDA with cetyl alcohol, so that lower amounts of DDA had a lower negative effect of particle size leading to smaller particle size when its concentration is decreased in the SLNs (Figure 2). For SA containing SLNs, increase in cetyl alcohol/amine ratio caused a slight increase in particle size, but the changes were not significant (Figure 2).

It could be understood that SA had more effects upon particle size reduction, when used with the 1 : 1 ratio with the lipid (Figure 2). In spite of what is reported in other studies that higher percentages of the organic/aqueous phase could decrease particle size [31], in the present study it was seen that regardless of the type of the amine type used, the organic/aqueous phase ratio did not have a significant effect upon particle size of the SLNs (Figure 3). The reason could be a high effect of the amine type and lipid/amine ratio on the particle size that overcasts the effect of this variable (Figure 2). The most effective variables on the particle size of nontargeted SLNs were amine type and cetyl alcohol/amine ratio (Figure 3).

3.1.2. HA Targeted SLNs. As Table 3 indicates coating of SLNs increased their particle size significantly. Among the targeted SLNs the formulations of $C_2L_3SO_{10}$ and $C_1L_{1.5}DO_{20}$ had the smallest and greatest particle sizes, respectively (Table 3). SA containing SLNs had smaller size than those prepared from DDA (Figure 4). This could be probably because of two reasons: first their nontargeted nanoparticles containing SA are smaller in size than DDA containing SLNs and secondly SA containing SLNs have less ability for creating electrostatic interaction with surface coated HA molecules. This is because the longer hydrocarbon chain of SA exerts a less electronegativity on the amine group compared to the lower chain length of DDA and consequently the amine group of DDA is more positive than SA and possibly can cause more effective electrostatic interactions with the surface HA molecules.

The effect of increasing of cetyl alcohol/amine ratio in both types of targeted SLNs containing SA and DDA was similar to nontargeted SLNs (Figures 2 and 4) and could be justified by the same reasons mentioned before. Increase in lipid/HA ratio in both groups of SLNs prepared from SA and DDA caused reduction in particle size that was reasonably

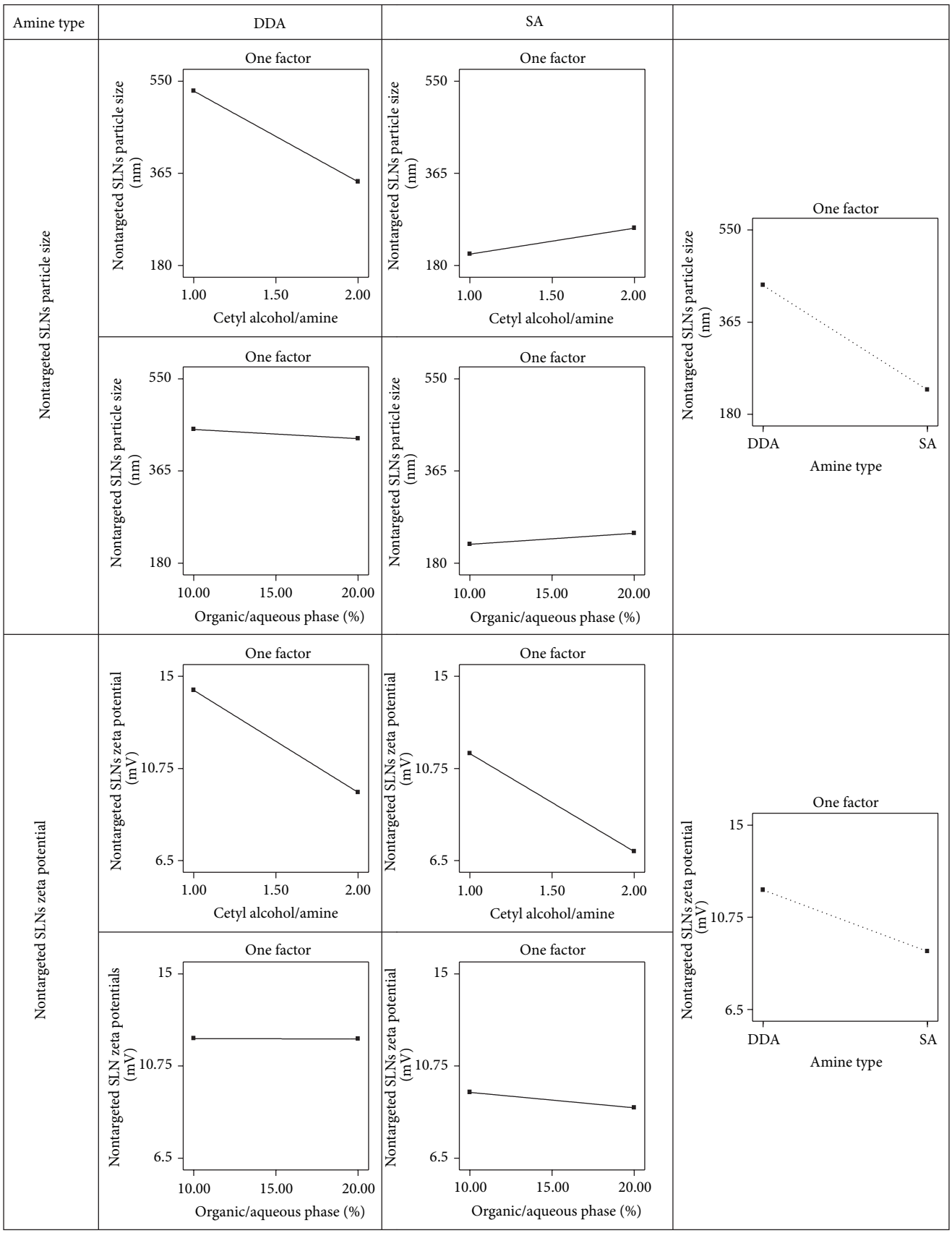

Figure 2: Effect of studied variables on particle size and zeta potential of nontargeted SLNs.

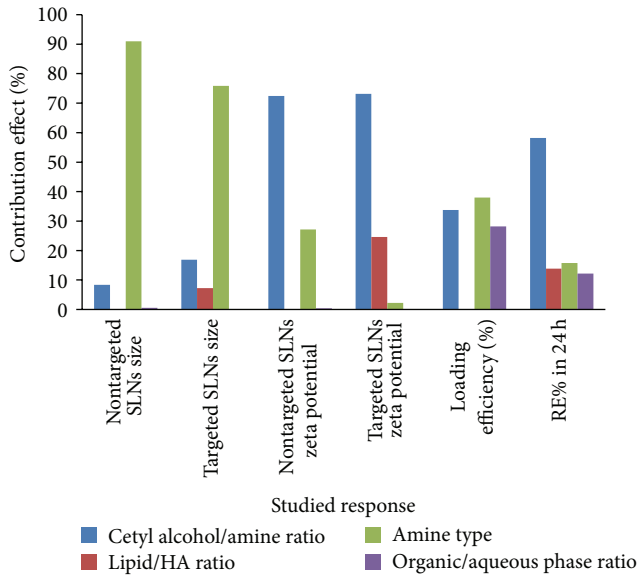

Figure 3: Contribution percent of studied variables on responses of nontargeted and HA targeted SLNs of etoposide.

Table 4: Zeta potential of nontargeted and HA targeted SLNs of etoposide ($n = 3$).

Formulation code	Nontargeted (mV) ± SD	HA targeted (mV) ± SD
$C_2L_{1.5}DO_{20}$	9.21 ± 0.53	−3.82 ± 0.65
$C_1L_3SO_{20}$	10.86 ± 0.73	−7.57 ± 0.82
$C_1L_3DO_{20}$	14.80 ± 0.94	−8.25 ± 0.78
$C_2L_3DO_{10}$	10.10 ± 0.46	−1.35 ± 0.58
$C_1L_3SO_{10}$	10.54 ± 0.59	−7.29 ± 0.75
$C_1L_{1.5}SO_{10}$	12.00 ± 0.42	−12.39 ± 0.64
$C_1L_{1.5}DO_{20}$	14.94 ± 0.91	−13.74 ± 0.98
$C_2L_{1.5}SO_{20}$	6.56 ± 0.86	−7.82 ± 0.95
$C_1L_{1.5}DO_{10}$	13.90 ± 0.89	−12.68 ± 0.92
$C_2L_3DO_{20}$	9.02 ± 0.38	−2.85 ± 0.72
$C_2L_3SO_{10}$	7.29 ± 0.82	−2.21 ± 0.96
$C_2L_{1.5}SO_{10}$	8.30 ± 0.65	−6.86 ± 0.87

predictable as HA itself increased the particle size of SLNs (Table 3); consequently when it is decreased the particle size normally reduced (Figure 4). The most effective variables on the particle size of HA targeted SLNs were amine type and cetyl alcohol/amine ratio (Figure 3).

3.2. Zeta Potential of SLNs. Table 4 shows mean zeta potential for each formulation. This response is described for nontargeted and HA targeted SLNs separately as in Table 4.

3.2.1. Nontargeted SLNs. The formulations of $C_1L_{1.5}DO_{20}$ and $C_2L_{1.5}SO_{20}$ had the largest and the smallest values of zeta potential, respectively (Table 4). The zeta potential of SA containing SLNs was lower than that of DDA ones (Figure 2), probably due to the reasons aforementioned already that SA has less ability to produce hydrogen bond with HA and consequently the more free amine groups imparting positive charge to the SLNs. Also, in both types of the amines, increase in cetyl alcohol/amine ratio caused decreases in zeta potential (Figure 2) which is reasonably predictable as the amine content of SLNs donates them the positive surface charge and when its amount is reduced the absolute value of zeta potential is also decreased. In addition, increase in percentage of the organic/aqueous phase in both types of amines did not have a significant effect upon zeta potential (Figure 2). This variable was not effective on the particle size of SLNs too (Figure 2). The most effective variables on the zeta potential of nontargeted SLNs were amine type and cetyl alcohol/amine ratio (Figure 3).

Table 5: Etoposide loading and release efficiency percent in 24 hours from HA targeted SLNs ($n = 3$).

Formulation code	Loading efficiency (%)	RE_{24} (%)
$C_2L_{1.5}DO_{20}$	54.76 ± 5.71	52.89 ± 7.06
$C_1L_3SO_{20}$	59.76 ± 3.22	65.05 ± 4.11
$C_1L_3DO_{20}$	42.56 ± 6.32	59.71 ± 8.17
$C_2L_3DO_{10}$	58.31 ± 8.79	57.49 ± 6.92
$C_1L_3SO_{10}$	65.70 ± 5.36	69.06 ± 5.62
$C_1L_{1.5}SO_{10}$	66.58 ± 4.56	65.36 ± 4.53
$C_1L_{1.5}DO_{20}$	39.53 ± 7.16	55.22 ± 7.86
$C_2L_{1.5}SO_{20}$	37.84 ± 6.19	54.47 ± 7.26
$C_1L_{1.5}DO_{10}$	40.66 ± 5.52	59.71 ± 6.44
$C_2L_3DO_{20}$	53.55 ± 8.49	54.24 ± 7.39
$C_2L_3SO_{10}$	43.72 ± 8.27	59.28 ± 6.83
$C_2L_{1.5}SO_{10}$	41.93 ± 4.95	55.35 ± 5.92

3.2.2. HA Targeted SLNs. The formulations of $C_2L_3DO_{10}$ and $C_1L_{1.5}DO_{20}$ had the largest and the smallest values of zeta potential among the targeted SLNs, respectively (Table 4). In both groups of targeted SLNs containing SA or DDA, increase in cetyl alcohol/amine ratio led to more positive zeta potential (Figure 4). This means that as much as the amine content was lower, the HA binding was lower too, and as HA imparted negative charge to the SLNs then its decrease in turn lowered the absolute value of zeta potential of SLNs. Increase in lipid/HA ratio increased the zeta potential (Figure 4) which is related to lower binding of HA in its lower concentration on the surface of nanoparticles. In addition, changing the amine type from DDA to SA caused induction of more negative zeta potential in SLNs (Figure 4). This might be due to that the zeta potential of SA containing nontargeted SLNs themselves was less than DDA ones (Figure 2); therefore, even after HA coating this value was still lower than DDA SLNs. The most effective variables on the zeta potential of HA targeted SLNs were cetyl alcohol/amine and also the lipid/HA ratio (Figure 3).

3.3. Loading Efficiency and Release Efficiency Percent. Table 5 shows the results of loading efficiency percent and 24-hour

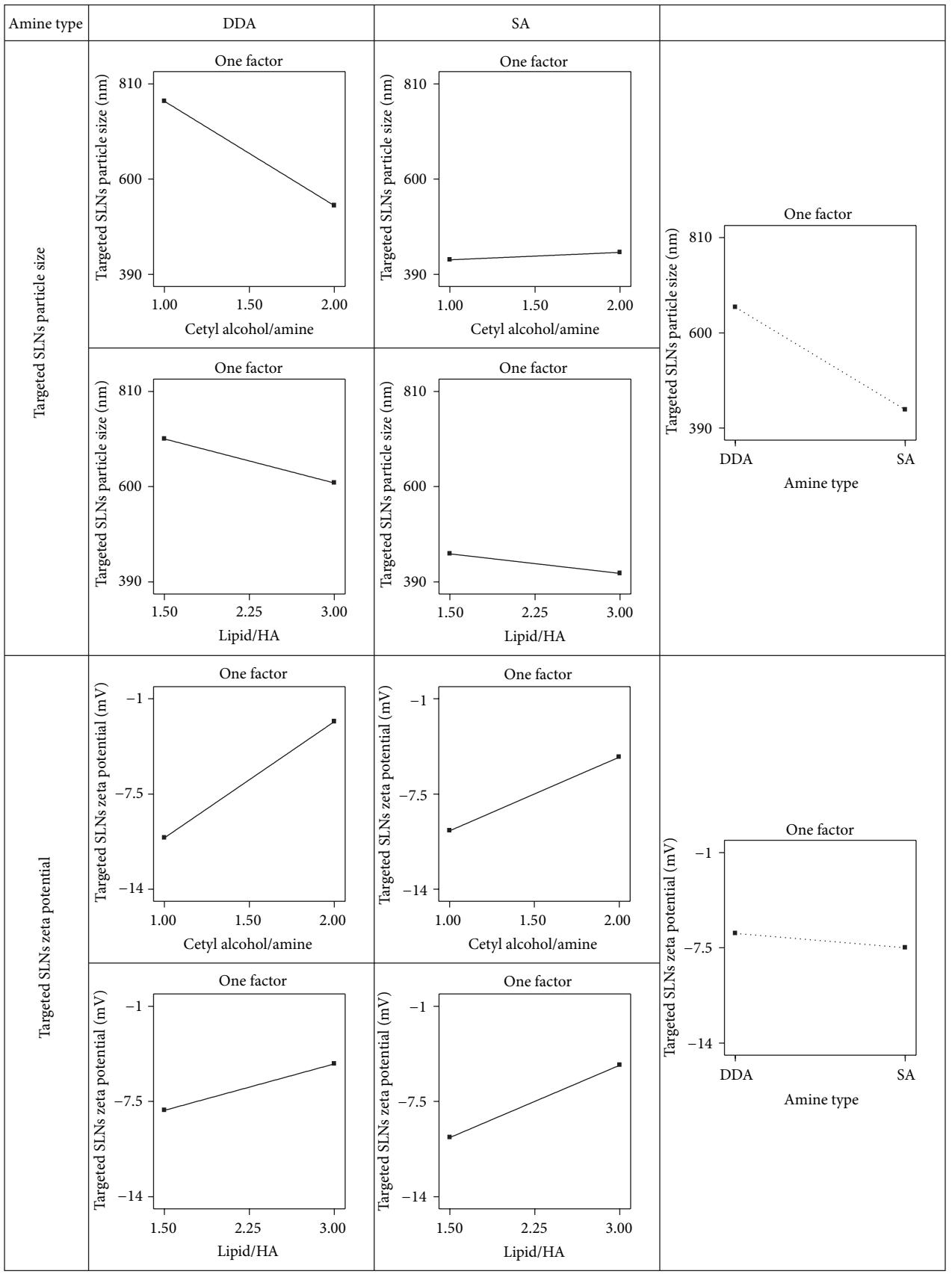

Figure 4: Effect of studied variables on particle size and zeta potential of HA targeted SLNs.

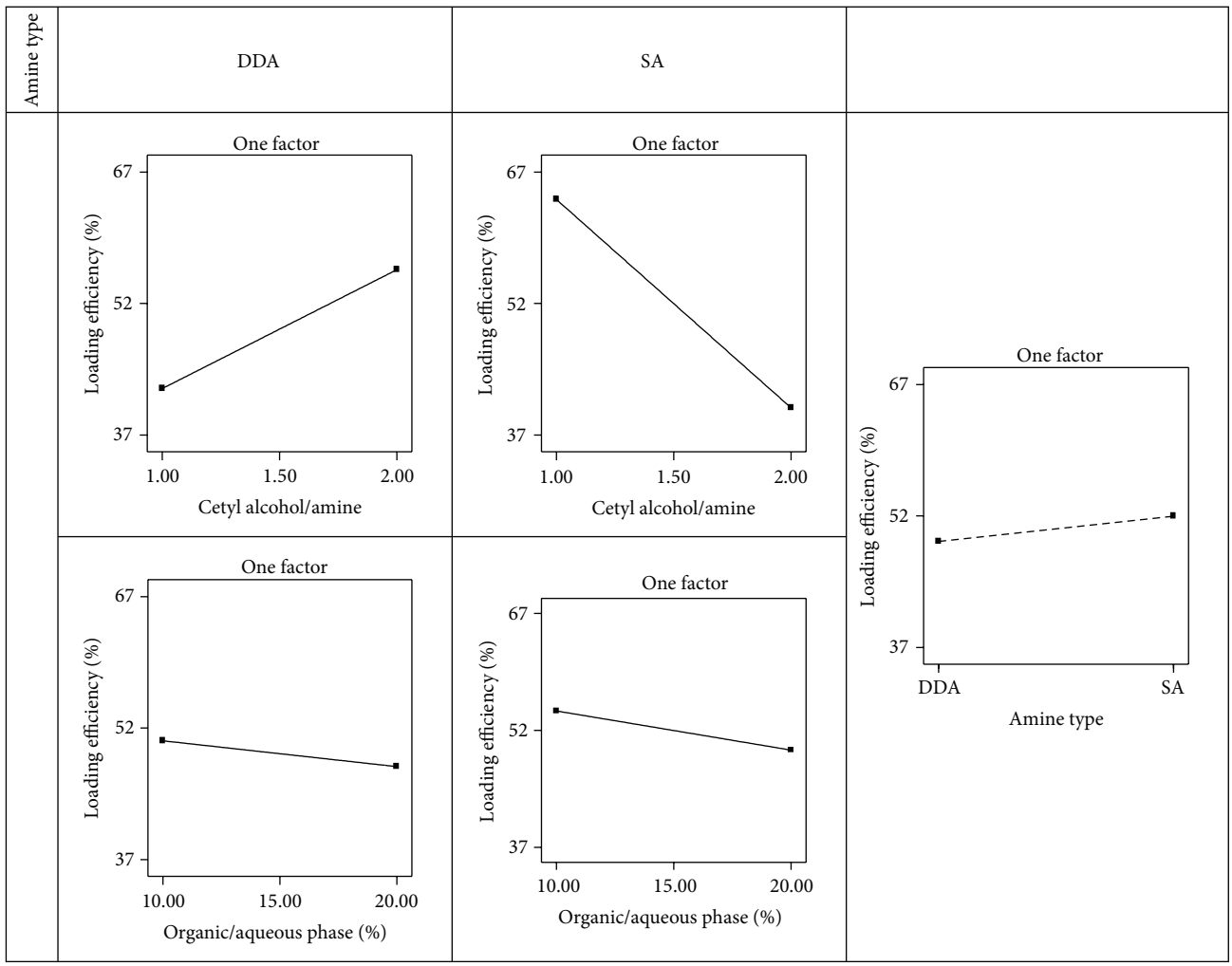

Figure 5: Effect of studied variables on etoposide loading efficiency percent in HA targeted SLNs.

release efficiency percent for each formulation of HA targeted SLNs.

3.3.1. Drug Loading Efficiency Percent. The formulations of $C_2L_{1.5}SO_{20}$ and $C_1L_{1.5}SO_{10}$ had the least and the highest etoposide loading efficiency percent, respectively (Table 5). Changing the amine type from DDA to SA led to increase in the loading efficiency percent of the SLNs (Figure 5). The reason could be better miscibility of SA in the structure of SLNs that made them able to trap more amounts of drug, in addition to having a more integrated layer of lipid in their wall. Wani et al. [32] study verifies effectiveness of functional groups located on the nanoparticles surface upon drug loading and release efficiency. Their results demonstrated that loading of mitoxantrone depended strongly on the type of surface functional groups in nanoparticles. Drug release was also strongly dependent on the pH of the release medium and the type of surface functional groups. No significant effect of surface modification of nanoparticles on particle toxicity was observed and the loaded drug exhibited comparable anticancer activity *in vitro* as the free drug.

In DDA SLNs, increase in the cetyl alcohol/amine ratio (or reduction of DDA which increases the ratio of cetyl alcohol/amine amount) increased drug loading efficiency percent (Figure 5) which expresses the negative effect of DDA upon loading, while this effect was reciprocal in the SA SLNs; that is, more amounts of SA caused more loading of the drug in SLNs (Figure 5). This effect is also shown in Figure 5 that changing the amine type from DDA to SA increased the drug loading in SLNs. The current results are consistent with the results obtained by Castro et al. [33] and could be related to the dispersing and surface activity properties of SA fatty amine, which facilitates stabilizing of the dispersion of the SLNs. Figure 4 also showed that SA containing SLNs had smaller size than those prepared from DDA. This causes a higher surface area for the nanoparticles and better contact with the drug molecules to be loaded in the SLNs. Increasing percentage of the organic/aqueous phase in both groups of SLNs containing SA or DDA led to enhanced drug loading (Figure 5), which could be justified as the higher the organic phase, the higher the content of SLNs components that are able to produce nanoparticles with more drug loading

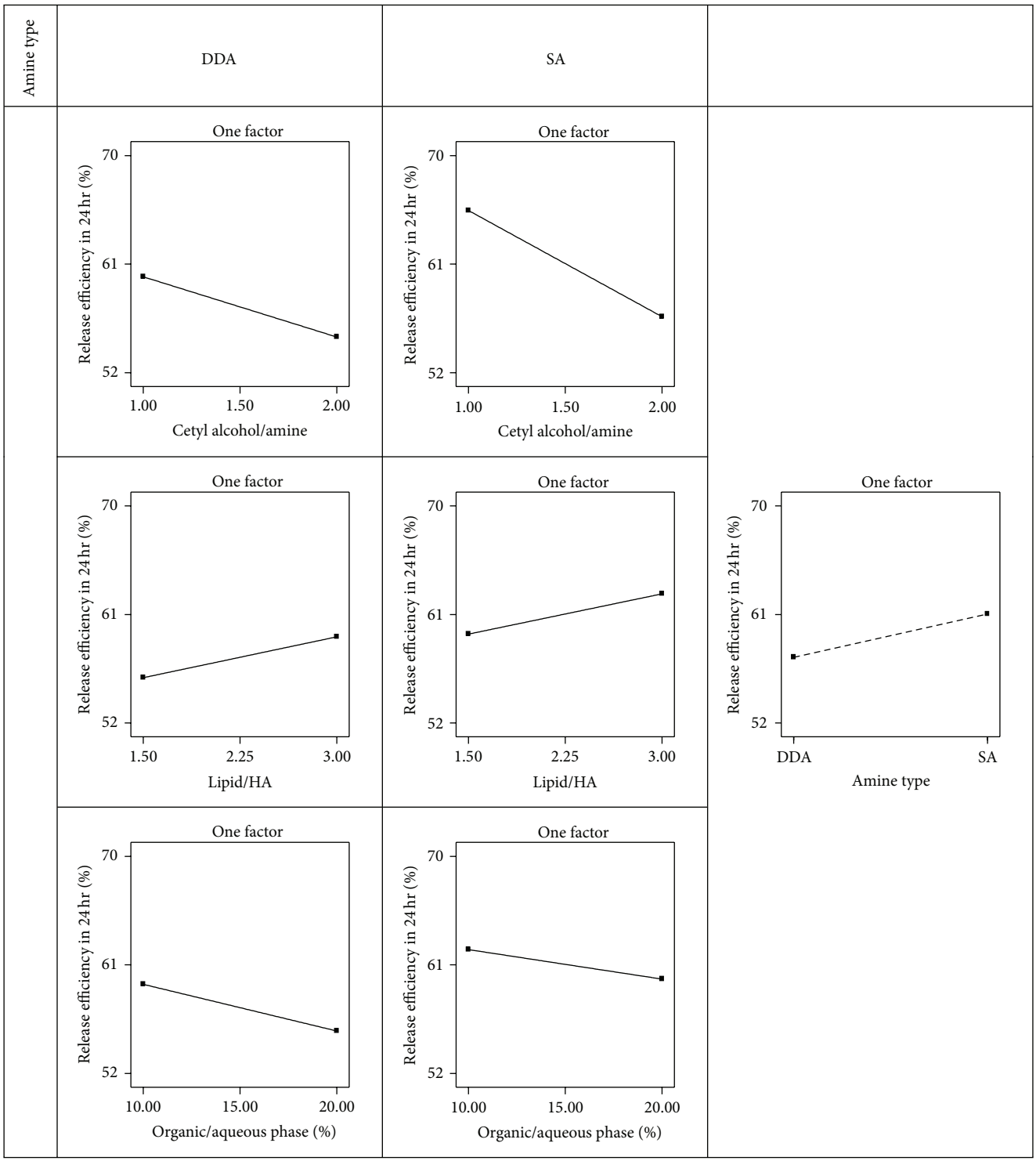

Figure 6: Effect of studied variables on etoposide release efficiency percent in 24 h from HA targeted SLNs.

efficiency (Figure 5). The most effective variables on the drug loading efficiency in HA targeted SLNs were amine type, cetyl alcohol/amine ratio, and organic/aqueous phase ratio (Figure 3).

3.3.2. Release Efficiency Percent in 24 Hours. The formulations of $C_2L_{1.5}DO_{20}$ and $C_1L_3SO_{10}$ had the lowest and the highest release efficiencies, respectively (Table 5). As Figure 6 indicates drug release efficiency from SA SLNs was higher than DDA ones. Regardless of the amine type used, in both groups of SLNs, increase in cetyl alcohol/amine ratio caused less drug release efficiency (Figure 6), which may be interpreted so that more amounts of amine existing in nanoparticles structure caused less integrity in the wall of

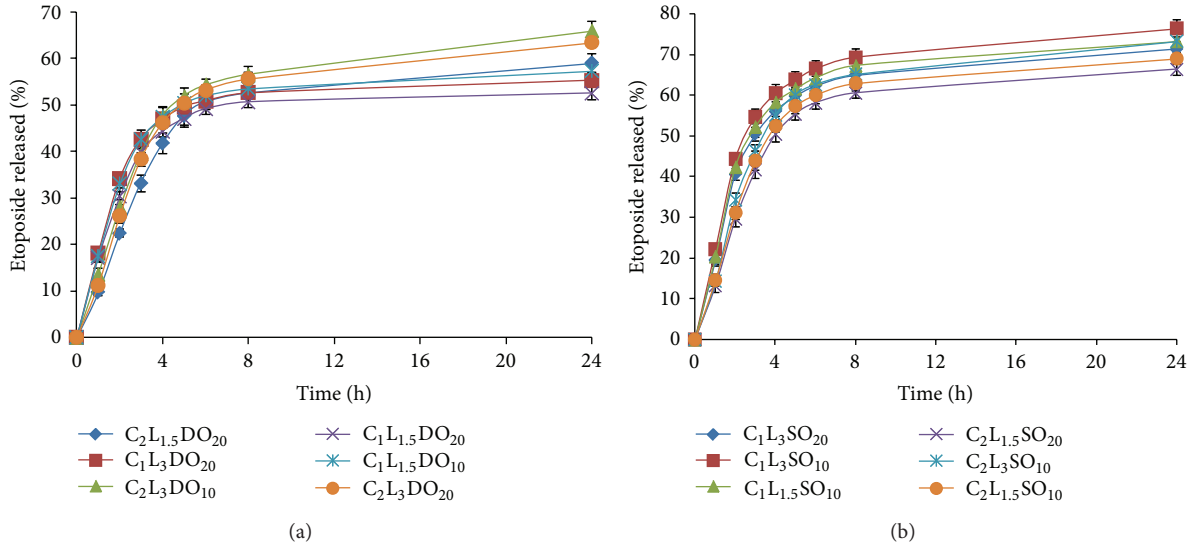

Figure 7: Etoposide release profiles from different HA targeted SLNs of (a) dodecylamine and (b) stearylamine.

SLNs and consequently easier release of the drug would happen. Increase in lipid/HA ratio caused more drug release efficiency (Figure 6) because the presence of more amounts of HA on the surface of nanoparticles made an additional barrier against drug release. Drug release from smaller nanoparticles is faster since they have a shorter path for drug molecules to pass and also the bigger surface area [34]. Hossann et al. [35] showed that a slight change in particle size caused a remarkable effect upon the features of the releasing drug from liposomes. According to the results of Table 4, the smallest and the biggest particle sizes of HA targeted SLNs belonged to SA SLNs and DDA ones, respectively. These findings are exactly consistent with the results of the drug release efficiency too (Figure 6).

The physicochemical properties of the drug are of the most important factors in the drug release rate through nanoparticles [36]. In other words, the high drug release rate in SA SLNs could be related to less electrostatic interaction between the etoposide and SA molecules (in comparison to more polar DDA molecules), which caused lower tendency of the drug for remaining in the core of nanoparticles. The reason of less interaction of the drug with SA is possibly, as mentioned before, the higher chain length of the SA, which has a less electronegativity effect on the amine group of this fatty amine and, consequently, the positive charge of the amine group in SA is weaker than DDA to bind with the drug through hydrogen bond and other interactions. Furthermore, nanoparticles, which had been produced with higher organic/aqueous phase percent, showed less drug release efficiency (Figure 6).

The most effective variable on the RE_{24}% of the HA targeted SLNs was cetyl alcohol/amine ratio and other variables had an equal effect on this response (Figure 3).

Etoposide release profiles from different HA targeted SLNs of dodecylamine and stearylamine are shown in Figures 7(a) and 7(b), respectively. As this figure shows SLNs prepared with stearylamine (Figure 7(b)) released the drug almost faster than those prepared from dodecylamine (Figure 7(a)). Generally the highest release percent ($P < 0.05$) in dodecylamine SLNs was seen in $C_2L_3DO_{10}$ and $C_2L_3DO_{20}$ nanoparticles while $C_1L_{1.5}DO_{20}$ SLNs showed the least release percent in this group ($P < 0.05$). However, in stearylamine containing nanoparticles (Figure 7(b)) $C_2L_{1.5}SO_{20}$ showed the slowest release rate ($P < 0.05$) compared to other stearylamine containing SLNs while $C_1L_3SO_{10}$ and $C_1L_{1.5}SO_{10}$ released their drug faster than others in this group ($P < 0.05$).

3.4. Optimization of the SLNs Formulation. The optimization was conducted by the Design-Expert software according to the gained responses discussed earlier. The suggesting formulation by the software with desirability of 86.8% was a formulation prepared using SA as amine type, cetyl alcohol/amine ratio of 1 : 1, lipid/HA ratio equal to 1.5 : 1, and organic/aqueous phase percent equal to 10%. This situation proposed by the software is in accordance with the formulation of $C_1L_{1.5}SO_{10}$.

The predicted and actual values of responses for this formulation are compared in Table 6. As this table indicates the design has been successful in predicting the responses and in all cases the differences between the predicted and actual values are less than 4%.

The optimized formulation containing HA was compared with those lacking coating. The particle size of these SLNs was 170.3 nm before coating and was enhanced to 416.42 nm after HA coating. Zeta potential of these SLNs was also 11.94 mV which changed to −12.65 mV after coating with HA. Drug release profile from the optimum formulation has been shown in Figure 7 and as indicated the SLNs released about 80% of the drug within 24 hours with release efficiency of 65.47% (Table 6).

Table 6: Comparison of predicted values of different responses by Design-Expert software and their actual values.

Responses	Particle size (nm)	Zeta potential (mV)	Drug loading efficiency (%)	RE_{24} (%)
Predicted	403.96	−12.99	65.76	64.94
Actual	416.42 ± 31.85	−12.65 ± 0.49	64.92 ± 3.76	65.47 ± 4.68
Error %	3.08	2.62	−1.28	0.82

Table 7: The results of elemental analysis of nontargeted and HA targeted SLNs.

SLN type	Elements %		
	C	H	N
Nontargeted SLNs	63.63 ± 0.03	10.31 ± 0.01	0.60 ± 0.00
HA targeted SLNs	62.10 ± 0.05	9.94 ± 0.01	0.85 ± 0.00

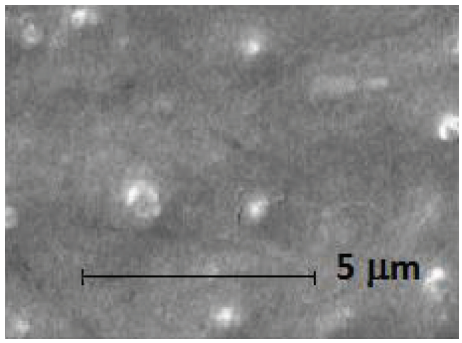

Figure 8: SEM image of HA coated $C_1L_{1.5}SO_{10}$ nanoparticles as the optimized SLNs.

The morphology of the optimized HA coated SLNs is seen in Figure 8. The SLNs show spherical shape with mean particle size as the results reported by DLS method.

3.5. Determining the Efficacy of the HA Binding to the Optimized Nanoparticles. Results of the CHNS/O elemental analysis are seen in Table 7.

Based on the amount of C, H, and N (carbon, hydrogen, and nitrogen) percentage in the conjugate, the conjugation efficiency percent of HA attached per SLNs weight was determined. C, N, and H% of each conjugate were calculated based on the data found for uncoated SLNs plus the amount calculated for the percent of the HA molecules attached to the SLNs.Considering the calculated ratio of C/N ratio in different theoretical percentages of HA attached to the SLNs a polynomial equation was obtained and then by using the experimental ratio of C/N of CHN analysis the percent of HA was calculated to be about 55.89 percent of HA bound to the nanoparticles surface physically, which is a considerable percentage.

4. Conclusion

In conclusion, preparation of the HA targeted SLNs of etoposide using solvent diffusion method was optimized statistically by irregular fraction factorial design. The most desirable SLN formulation contained stearylamine, cetyl alcohol/amine ratio of 1 : 1, lipid/HA ratio equal to 1.5 : 1, and organic/aqueous phase percent of 10%. HA was coated successfully on the SLNs physically and about 55.89% of HA was attached to the nanoparticles. These SLNs had the particle size of 416.42 nm after HA coating, zeta potential of 12.65 mV, with release efficiency of 65.47% after 24 hours and drug loading efficiency was about 64.92%. This formulation seems promising from the physicochemical properties point of view and may be considered for further studies in drug targeting to ovarian cancer cells overexpressing CD44 receptors.

Conflict of Interests

The authors declare that there is no conflict of interests regarding the publication of this paper.

Acknowledgment

The authors would like to thank Vice Chancellor for Research of Isfahan University of Medical Sciences that accepted project finances.

References

[1] A. E. Guppy, P. D. Nathan, and G. J. S. Rustin, "Epithelial ovarian cancer: A review of current management," *Clinical Oncology*, vol. 17, no. 6, pp. 399–411, 2005.

[2] P. A. Radice, P. A. Bunn Jr., and D. C. Ihde, "Therapeutic trials with VP-16-213 and VM-26: active agents in small cell lung cancer, non-Hodgkin's lymphomas, and other malignancies," *Cancer Treatment Reports*, vol. 63, no. 8, pp. 1231–1239, 1979.

[3] F. Cabanillas, F. B. Hagemeister, G. P. Bodey, and E. J. Freireich, "IMVP-16: an effective regimen for patients with lymphoma who have relapsed after initial combination chemotherapy," *Blood*, vol. 60, no. 3, pp. 693–697, 1982.

[4] G. Mathe, L. Schwarzenberg, and P. Pouillart, "Two epipodophyllotoxin derivatives, VM 26 and VP 16213, in the treatment of leukemias, hematosarcomas, and lymphomas," *Cancer*, vol. 34, no. 4, pp. 985–992, 1974.

[5] A. D. Ho, T. Lipp, G. Ehninger et al., "Combination of mitoxantrone and etoposide in refractory acute myelogenous leukemia-an active and well-tolerated regimen," *Journal of Clinical Oncology*, vol. 6, no. 2, pp. 213–217, 1988.

[6] P. J. O'Dwyer, B. Leyland-Jones, and M. T. Alonso, "Etoposide (VP-16-213). Current status of an active anticancer drug," *The New England Journal of Medicine*, vol. 312, no. 11, pp. 692–700, 1985.

[7] R. E. Taylor, T. J. McElwain, A. Barrett, and M. J. Peckham, "Etoposide as a single agent in relapsed advanced lymphomas. A phase II study," *Cancer Chemotherapy and Pharmacology*, vol. 7, no. 2-3, pp. 175–177, 1982.

[8] H. Li, X. Zhao, Y. Ma, G. Zhai, L. Li, and H. Lou, "Enhancement of gastrointestinal absorption of quercetin by solid lipid

nanoparticles," *Journal of Controlled Release*, vol. 133, no. 3, pp. 238–244, 2009.

[9] M. Uner and G. Yener, "Importance of solid lipid nanoparticles (SLN) in various administration routes and future perspectives," *International Journal of Nanomedicine*, vol. 2, no. 3, pp. 289–300, 2007.

[10] S. Mukherjee, S. Ray, and R. S. Thakur, "Solid lipid nanoparticles: a modern formulation approach in drug delivery system," *Indian Journal of Pharmaceutical Sciences*, vol. 71, no. 4, pp. 349–358, 2009.

[11] W. Mehnert and K. Mader, "Solid lipid nanoparticles: production, characterization and applications," *Advanced Drug Delivery Reviews*, vol. 47, no. 2-3, pp. 165–196, 2001.

[12] R. H. Müller, K. Mäder, and S. Gohla, "Solid lipid nanoparticles (SLN) for controlled drug delivery—a review of the state of the art," *European Journal of Pharmaceutics and Biopharmaceutics*, vol. 50, no. 1, pp. 161–177, 2000.

[13] K. S. Yadav, K. Chuttani, A. K. Mishra, and K. K. Sawant, "Long circulating nanoparticles of etoposide using PLGA-MPEG and PLGA-pluronic block copolymers: characterization, drug-release, blood-clearance, and biodistribution studies," *Drug Development Research*, vol. 71, no. 4, pp. 228–239, 2010.

[14] L. H. Reddy, R. K. Sharma, K. Chuttani, A. K. Mishra, and R. R. Murthy, "Etoposide-incorporated tripalmitin nanoparticles with different surface charge: formulation, characterization, radiolabeling, and biodistribution studies," *The AAPS Journal*, vol. 6, no. 3, article e23, 2004.

[15] L. Harivardhan Reddy, R. K. Sharma, K. Chuttani, A. K. Mishra, and R. S. R. Murthy, "Influence of administration route on tumor uptake and biodistribution of etoposide loaded solid lipid nanoparticles in Dalton's lymphoma tumor bearing mice," *Journal of Controlled Release*, vol. 105, no. 3, pp. 185–198, 2005.

[16] G. Yordanov, R. Skrobanska, and A. Evangelatov, "Colloidal formulations of etoposide based on poly(butyl cyanoacrylate) nanoparticles: preparation, physicochemical properties and cytotoxicity," *Colloids and Surfaces B: Biointerfaces*, vol. 101, pp. 215–222, 2013.

[17] E. Kiliay, M. Demirbilek, M. Türk, E. Güven, B. Hazer, and E. B. Denkbas, "Preparation and characterization of poly(3-hydroxybutyrate-co-3- hydroxyhexanoate) (PHBHHX) based nanoparticles for targeted cancer therapy," *European Journal of Pharmaceutical Sciences*, vol. 44, no. 3, pp. 310–320, 2011.

[18] R. C. Savani, G. Cao, P. M. Pooler, A. Zaman, Z. Zhou, and H. M. DeLisser, "Differential involvement of the hyaluronan (HA) receptors CD44 and receptor for HA-mediated motility in endothelial cell function and angiogenesis," *Journal of Biological Chemistry*, vol. 276, no. 39, pp. 36770–36778, 2001.

[19] B. A. Nevius, Y. P. Chen, J. L. Ferry, and A. W. Decho, "Surface-functionalization effects on uptake of fluorescent polystyrene nanoparticles by model biofilms," *Ecotoxicology*, vol. 21, no. 8, pp. 2205–2213, 2012.

[20] G. Kremser, T. Rath, B. Kunert et al., "Structural characterisation of alkyl amine-capped zinc sulphide nanoparticles," *Journal of Colloid and Interface Science*, vol. 369, no. 1, pp. 154–159, 2012.

[21] Y. Sun, *Synthesis of gold-amine nanoparticles of various sizes using two different methods [M.S. thesis]*, Department of Chemistry, Kansas State University, 2010.

[22] Y. Luo, N. J. Bernshaw, Z. R. Lu, J. Kopecek, and G. D. Prestwich, "Targeted delivery of doxorubicin by HPMA copolymer-hyaluronan bioconjugates," *Pharmaceutical Research*, vol. 19, no. 4, pp. 396–402, 2002.

[23] K. Akima, H. Ito, Y. Iwata et al., "Evaluation of antitumor activities of hyaluronate binding antitumor drugs: synthesis, characterization and antitumor activity," *Journal of Drug Targeting*, vol. 4, no. 1, pp. 1–8, 1996.

[24] A. Rosato, A. Banzato, G. de Luca et al., "HYTAD1-p20: a new paclitaxel-hyaluronic acid hydrosoluble bioconjugate for treatment of superficial bladder cancer," *Urologic Oncology: Seminars and Original Investigations*, vol. 24, no. 3, pp. 207–215, 2006.

[25] D. Peer and R. Margalit, "Loading mitomycin C inside long circulating hyaluronan targeted nano-liposomes increases its antitumor activity in three mice tumor models," *International Journal of Cancer*, vol. 108, no. 5, pp. 780–789, 2004.

[26] H. Lee, H. Mok, S. Lee, Y. K. Oh, and T. G. Park, "Target-specific intracellular delivery of siRNA using degradable hyaluronic acid nanogels," *Journal of Controlled Release*, vol. 119, no. 2, pp. 245–252, 2007.

[27] Y. H. Yun, D. J. Goetz, P. Yellen, and W. Chen, "Hyaluronan microspheres for sustained gene delivery and site-specific targeting," *Biomaterials*, vol. 25, no. 1, pp. 147–157, 2004.

[28] J. Varshosaz, S. Eskandari, and M. Tabakhian, "Production and optimization of valproic acid nanostructured lipid carriers by the Taguchi design," *Pharmaceutical Development and Technology*, vol. 15, no. 1, pp. 89–96, 2010.

[29] Y. Ataman-Önal, S. Munier, A. Ganée et al., "Surfactant-free anionic PLA nanoparticles coated with HIV-1 p24 protein induced enhanced cellular and humoral immune responses in various animal models," *Journal of Controlled Release*, vol. 112, no. 2, pp. 175–185, 2006.

[30] V. Teeranachaideekul, E. B. Souto, V. B. Junyaprasert, and R. H. Müller, "Cetyl palmitate-based NLC for topical delivery of Coenzyme Q10: development, physicochemical characterization and in vitro release studies," *European Journal of Pharmaceutics and Biopharmaceutics*, vol. 67, no. 1, pp. 141–148, 2007.

[31] R. M. Mainardes and R. C. Evangelista, "PLGA nanoparticles containing praziquantel: effect of formulation variables on size distribution," *International Journal of Pharmaceutics*, vol. 290, no. 1-2, pp. 137–144, 2005.

[32] A. Wani, E. Muthuswamy, G. H. L. Savithra, G. Mao, S. Brock, and D. Oupický, "Surface functionalization of mesoporous silica nanoparticles controls loading and release behavior of mitoxantrone," *Pharmaceutical Research*, vol. 29, no. 9, pp. 2407–2418, 2012.

[33] G. A. Castro, A. L. Coelho, C. A. Oliveira, G. A. B. Mahecha, R. L. Oréfice, and L. A. M. Ferreira, "Formation of ion pairing as an alternative to improve encapsulation and stability and to reduce skin irritation of retinoic acid loaded in solid lipid nanoparticles," *International Journal of Pharmaceutics*, vol. 381, no. 1, pp. 77–83, 2009.

[34] Y. Zhao, M. B. Brown, and S. A. Jones, "The effects of particle properties on nanoparticle drug retention and release in dynamic minoxidil foams," *International Journal of Pharmaceutics*, vol. 383, no. 1-2, pp. 277–284, 2010.

[35] M. Hossann, T. Wang, M. Wiggenhorn et al., "Size of thermosensitive liposomes influences content release," *Journal of Controlled Release*, vol. 147, no. 3, pp. 436–443, 2010.

[36] M. M. A. Abdel-Mottaleb, D. Neumann, and A. Lamprecht, "In vitro drug release mechanism from lipid nanocapsules (LNC)," *International Journal of Pharmaceutics*, vol. 390, no. 2, pp. 208–213, 2010.